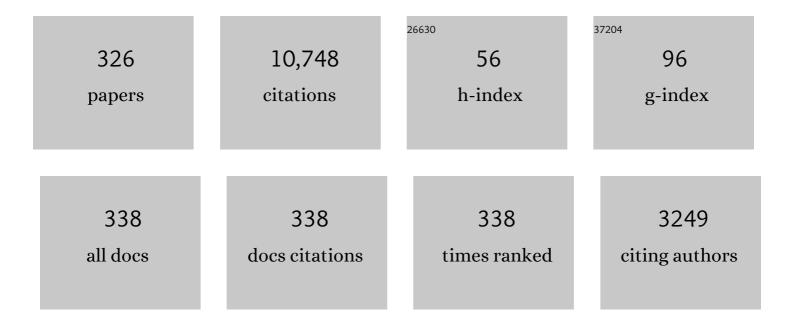
## Chao Zuo

## List of Publications by Year in descending order

Source: https://exaly.com/author-pdf/3094854/publications.pdf Version: 2024-02-01



#	Article	IF	CITATIONS
1	Phase shifting algorithms for fringe projection profilometry: A review. Optics and Lasers in Engineering, 2018, 109, 23-59.	3.8	728
2	Temporal phase unwrapping algorithms for fringe projection profilometry: A comparative review. Optics and Lasers in Engineering, 2016, 85, 84-103.	3.8	666
3	High-speed three-dimensional shape measurement for dynamic scenes using bi-frequency tripolar pulse-width-modulation fringe projection. Optics and Lasers in Engineering, 2013, 51, 953-960.	3.8	300
4	Transport of intensity equation: a tutorial. Optics and Lasers in Engineering, 2020, 135, 106187.	3.8	272
5	Transport of intensity phase retrieval and computational imaging for partially coherent fields: The phase space perspective. Optics and Lasers in Engineering, 2015, 71, 20-32.	3.8	268
6	High-resolution transport-of-intensity quantitative phase microscopy with annular illumination. Scientific Reports, 2017, 7, 7654.	3.3	256
7	Fringe pattern analysis using deep learning. Advanced Photonics, 2019, 1, 1.	11.8	248
8	Deep learning in optical metrology: a review. Light: Science and Applications, 2022, 11, 39.	16.6	214
9	High-speed three-dimensional profilometry for multiple objects with complex shapes. Optics Express, 2012, 20, 19493.	3.4	201
10	Micro Fourier Transform Profilometry (μFTP): 3D shape measurement at 10,000 frames per second. Optics and Lasers in Engineering, 2018, 102, 70-91.	3.8	186
11	High-speed transport-of-intensity phase microscopy with an electrically tunable lens. Optics Express, 2013, 21, 24060.	3.4	172
12	Adaptive step-size strategy for noise-robust Fourier ptychographic microscopy. Optics Express, 2016, 24, 20724.	3.4	164
13	Microscopic fringe projection profilometry: A review. Optics and Lasers in Engineering, 2020, 135, 106192.	3.8	163
14	General solution for high dynamic range three-dimensional shape measurement using the fringe projection technique. Optics and Lasers in Engineering, 2014, 59, 56-71.	3.8	156
15	Real-time 3-D shape measurement with composite phase-shifting fringes and multi-view system. Optics Express, 2016, 24, 20253.	3.4	155
16	Review of phase measuring deflectometry. Optics and Lasers in Engineering, 2018, 107, 247-257.	3.8	152
17	Deep-learning-enabled geometric constraints and phase unwrapping for single-shot absolute 3D shape measurement. APL Photonics, 2020, 5, .	5.7	146
18	High dynamic range 3D measurements with fringe projection profilometry: a review. Measurement Science and Technology, 2018, 29, 122001.	2.6	145

#	Article	IF	CITATIONS
19	Robust dynamic 3-D measurements with motion-compensated phase-shifting profilometry. Optics and Lasers in Engineering, 2018, 103, 127-138.	3.8	141
20	Phase aberration compensation in digital holographic microscopy based on principal component analysis. Optics Letters, 2013, 38, 1724.	3.3	140
21	Single-shot absolute 3D shape measurement with deep-learning-based color fringe projection profilometry. Optics Letters, 2020, 45, 1842.	3.3	139
22	Efficient positional misalignment correction method for Fourier ptychographic microscopy. Biomedical Optics Express, 2016, 7, 1336.	2.9	134
23	Calibration of fringe projection profilometry: A comparative review. Optics and Lasers in Engineering, 2021, 143, 106622.	3.8	130
24	Transport-of-intensity phase imaging using Savitzky-Golay differentiation filter - theory and applications. Optics Express, 2013, 21, 5346.	3.4	129
25	Noninterferometric single-shot quantitative phase microscopy. Optics Letters, 2013, 38, 3538.	3.3	128
26	Wide-field high-resolution 3D microscopy with Fourier ptychographic diffraction tomography. Optics and Lasers in Engineering, 2020, 128, 106003.	3.8	122
27	Optimized pulse width modulation pattern strategy for three-dimensional profilometry with projector defocusing. Applied Optics, 2012, 51, 4477.	1.8	120
28	Range Limited Bi-Histogram Equalization for image contrast enhancement. Optik, 2013, 124, 425-431.	2.9	110
29	Resolution Analysis in a Lens-Free On-Chip Digital Holographic Microscope. IEEE Transactions on Computational Imaging, 2020, 6, 697-710.	4.4	107
30	On a universal solution to the transport-of-intensity equation. Optics Letters, 2020, 45, 3649.	3.3	102
31	High-speed in vitro intensity diffraction tomography. Advanced Photonics, 2019, 1, 1.	11.8	100
32	Boundary-artifact-free phase retrieval with the transport of intensity equation: fast solution with use of discrete cosine transform. Optics Express, 2014, 22, 9220.	3.4	99
33	Lensless phase microscopy and diffraction tomography with multi-angle and multi-wavelength illuminations using a LED matrix. Optics Express, 2015, 23, 14314.	3.4	94
34	Scene-based nonuniformity correction algorithm based on interframe registration. Journal of the Optical Society of America A: Optics and Image Science, and Vision, 2011, 28, 1164.	1.5	92
35	High-speed 3D shape measurement using the optimized composite fringe patterns and stereo-assisted structured light system. Optics Express, 2019, 27, 2411.	3.4	92
36	Robust Chemical Synthesis of Membrane Proteins through a General Method of Removable Backbone Modification. Journal of the American Chemical Society, 2016, 138, 3553-3561.	13.7	88

#	Article	IF	CITATIONS
37	Sampling criteria for Fourier ptychographic microscopy in object space and frequency space. Optics Express, 2016, 24, 15765.	3.4	85
38	Comparison of two-dimensional integration methods for shape reconstruction from gradient data. Optics and Lasers in Engineering, 2015, 64, 1-11.	3.8	83
39	Resolution-enhanced Fourier ptychographic microscopy based on high-numerical-aperture illuminations. Scientific Reports, 2017, 7, 1187.	3.3	82
40	Robust and efficient multi-frequency temporal phase unwrapping: optimal fringe frequency and pattern sequence selection. Optics Express, 2017, 25, 20381.	3.4	81
41	Temporal phase unwrapping using deep learning. Scientific Reports, 2019, 9, 20175.	3.3	81
42	High-speed three-dimensional shape measurement based on cyclic complementary Gray-code light. Optics Express, 2019, 27, 1283.	3.4	79
43	High-resolution and large field-of-view Fourier ptychographic microscopy and its applications in biomedicine. Reports on Progress in Physics, 2020, 83, 096101.	20.1	76
44	A new microscopic telecentric stereo vision system - Calibration, rectification, and three-dimensional reconstruction. Optics and Lasers in Engineering, 2019, 113, 14-22.	3.8	74
45	Display and detail enhancement for high-dynamic-range infrared images. Optical Engineering, 2011, 50, 1.	1.0	72
46	Micro deep learning profilometry for high-speed 3D surface imaging. Optics and Lasers in Engineering, 2019, 121, 416-427.	3.8	71
47	Transport of intensity diffraction tomography with non-interferometric synthetic aperture for three-dimensional label-free microscopy. Light: Science and Applications, 2022, 11, .	16.6	70
48	Single-shot quantitative phase microscopy based on color-multiplexed Fourier ptychography. Optics Letters, 2018, 43, 3365.	3.3	69
49	Generalized framework for non-sinusoidal fringe analysis using deep learning. Photonics Research, 2021, 9, 1084.	7.0	69
50	miR-335-5p targeting ICAM-1 inhibits invasion and metastasis of thyroid cancer cells. Biomedicine and Pharmacotherapy, 2018, 106, 983-990.	5.6	63
51	Deep-learning-enabled dual-frequency composite fringe projection profilometry for single-shot absolute 3D shape measurement. Opto-Electronic Advances, 2022, 5, 210021-210021.	13.3	63
52	Dynamic 3-D measurement based on fringe-to-fringe transformation using deep learning. Optics Express, 2020, 28, 9405.	3.4	62
53	New temporal high-pass filter nonuniformity correction based on bilateral filter. Optical Review, 2011, 18, 197-202.	2.0	61
54	Adaptive pixel-super-resolved lensfree in-line digital holography for wide-field on-chip microscopy. Scientific Reports, 2017, 7, 11777.	3.3	61

#	Article	IF	CITATIONS
55	Fast three-dimensional measurements for dynamic scenes with shiny surfaces. Optics Communications, 2017, 382, 18-27.	2.1	61
56	Motion-artifact-free dynamic 3D shape measurement with hybrid Fourier-transform phase-shifting profilometry. Optics Express, 2019, 27, 2713.	3.4	59
57	High-speed Fourier ptychographic microscopy based on programmable annular illuminations. Scientific Reports, 2018, 8, 7669.	3.3	58
58	Smart computational light microscopes (SCLMs) of smart computational imaging laboratory (SCILab). PhotoniX, 2021, 2, .	13.5	56
59	Learning-based method to reconstruct complex targets through scattering medium beyond the memory effect. Optics Express, 2020, 28, 2433.	3.4	56
60	Optimal illumination scheme for isotropic quantitative differential phase contrast microscopy. Photonics Research, 2019, 7, 890.	7.0	53
61	High-speed high dynamic range 3D shape measurement based on deep learning. Optics and Lasers in Engineering, 2020, 134, 106245.	3.8	51
62	High-speed real-time 3D shape measurement based on adaptive depth constraint. Optics Express, 2018, 26, 22440.	3.4	49
63	High-speed three-dimensional shape measurement using geometry-constraint-based number-theoretical phase unwrapping. Optics and Lasers in Engineering, 2019, 115, 21-31.	3.8	48
64	Deep-learning-based fringe-pattern analysis with uncertainty estimation. Optica, 2021, 8, 1507.	9.3	48
65	High-resolution real-time 360Ű 3D model reconstruction of a handheld object with fringe projection profilometry. Optics Letters, 2019, 44, 5751.	3.3	47
66	Three-dimensional tomographic microscopy technique with multi-frequency combination with partially coherent illuminations. Biomedical Optics Express, 2018, 9, 2526.	2.9	46
67	Boundary-artifact-free phase retrieval with the transport of intensity equation II: applications to microlens characterization. Optics Express, 2014, 22, 18310.	3.4	45
68	Efficient quantitative phase microscopy using programmable annular LED illumination. Biomedical Optics Express, 2017, 8, 4687.	2.9	45
69	High-precision real-time 3D shape measurement using a bi-frequency scheme and multi-view system. Applied Optics, 2017, 56, 3646.	2.1	45
70	Phase retrieval using spatially modulated illumination. Optics Letters, 2014, 39, 3615.	3.3	44
71	Zonal wavefront reconstruction in quadrilateral geometry for phase measuring deflectometry. Applied Optics, 2017, 56, 5139.	2.1	43
72	Highly porous nickel oxide thin films prepared by a hydrothermal synthesis method for electrochromic application. Journal of Physics and Chemistry of Solids, 2013, 74, 1522-1526.	4.0	41

#	Article	IF	CITATIONS
73	Automatic identification and removal of outliers for high-speed fringe projection profilometry. Optical Engineering, 2013, 52, 013605.	1.0	41
74	High dynamic range 3D shape measurement based on the intensity response function of a camera. Applied Optics, 2018, 57, 1378.	1.8	41
75	Deep learning-based fringe modulation-enhancing method for accurate fringe projection profilometry. Optics Express, 2020, 28, 21692.	3.4	41
76	Absolute three-dimensional micro surface profile measurement based on a Greenough-type stereomicroscope. Measurement Science and Technology, 2017, 28, 045004.	2.6	40
77	Phase discrepancy analysis and compensation for fast Fourier transform based solution of the transport of intensity equation. Optics Express, 2014, 22, 17172.	3.4	39
78	Improved intensity-optimized dithering technique for 3D shape measurement. Optics and Lasers in Engineering, 2015, 66, 158-164.	3.8	39
79	Spline based least squares integration for two-dimensional shape or wavefront reconstruction. Optics and Lasers in Engineering, 2017, 91, 221-226.	3.8	39
80	Single-shot 3D shape measurement using an end-to-end stereo matching network for speckle projection profilometry. Optics Express, 2021, 29, 13388.	3.4	39
81	Composite fringe projection deep learning profilometry for single-shot absolute 3D shape measurement. Optics Express, 2022, 30, 3424.	3.4	38
82	High-speed real-time 3-D coordinates measurement based on fringe projection profilometry considering camera lens distortion. Optics Communications, 2014, 329, 44-56.	2.1	36
83	Phase retrieval with the transport-of-intensity equation in an arbitrarily shaped aperture by iterative discrete cosine transforms. Optics Letters, 2015, 40, 1976.	3.3	36
84	Vignetting effect in Fourier ptychographic microscopy. Optics and Lasers in Engineering, 2019, 120, 40-48.	3.8	36
85	High-resolution real-time 360â~ 3D surface defect inspection with fringe projection profilometry. Optics and Lasers in Engineering, 2021, 137, 106382.	3.8	35
86	Direct continuous phase demodulation in digital holography with use of the transport-of-intensity equation. Optics Communications, 2013, 309, 221-226.	2.1	34
87	Graphics processing unit–assisted real-time three-dimensional measurement using speckle-embedded fringe. Applied Optics, 2015, 54, 6865.	2.1	34
88	Programmable aperture microscopy: A computational method for multi-modal phase contrast and light field imaging. Optics and Lasers in Engineering, 2016, 80, 24-31.	3.8	34
89	Adaptive denoising method for Fourier ptychographic microscopy. Optics Communications, 2017, 404, 23-31.	2.1	34
90	Variational Hilbert Quantitative Phase Imaging. Scientific Reports, 2020, 10, 13955.	3.3	34

#	Article	IF	CITATIONS
91	Regional cerebral metabolism alterations affect resting-state functional connectivity in major depressive disorder. Quantitative Imaging in Medicine and Surgery, 2018, 8, 910-924.	2.0	33
92	Optimal principal component analysis-based numerical phase aberration compensation method for digital holography. Optics Letters, 2016, 41, 1293.	3.3	32
93	Wavelength-scanning lensfree on-chip microscopy for wide-field pixel-super-resolved quantitative phase imaging. Optics Letters, 2021, 46, 2023.	3.3	32
94	Optical diffraction tomography microscopy with transport of intensity equation using a light-emitting diode array. Optics and Lasers in Engineering, 2017, 95, 26-34.	3.8	31
95	Real-time high dynamic range 3D measurement using fringe projection. Optics Express, 2020, 28, 24363.	3.4	30
96	Lensfree dynamic super-resolved phase imaging based on active micro-scanning. Optics Letters, 2018, 43, 3714.	3.3	29
97	Single-shot isotropic quantitative phase microscopy based on color-multiplexed differential phase contrast. APL Photonics, 2019, 4, 121301.	5.7	29
98	Calibration method for panoramic 3D shape measurement with plane mirrors. Optics Express, 2019, 27, 36538.	3.4	28
99	Optimal illumination pattern for transport-of-intensity quantitative phase microscopy. Optics Express, 2018, 26, 27599.	3.4	27
100	Dynamic microscopic 3D shape measurement based on marker-embedded Fourier transform profilometry. Applied Optics, 2018, 57, 772.	1.8	27
101	Improved interframe registration based nonuniformity correction for focal plane arrays. Infrared Physics and Technology, 2012, 55, 263-269.	2.9	26
102	High-precision real-time 3D shape measurement based on a quad-camera system. Journal of Optics (United Kingdom), 2018, 20, 014009.	2.2	26
103	Microscopic 3D measurement of shiny surfaces based on a multi-frequency phase-shifting scheme. Optics and Lasers in Engineering, 2019, 122, 1-7.	3.8	25
104	Multimodal super-resolution reconstruction of infrared and visible images via deep learning. Optics and Lasers in Engineering, 2022, 156, 107078.	3.8	25
105	Shape reconstruction from gradient data in an arbitrarily-shaped aperture by iterative discrete cosine transforms in Southwell configuration. Optics and Lasers in Engineering, 2015, 67, 176-181.	3.8	24
106	Two-dimensional stitching interferometry for self-calibration of high-order additive systematic errors. Optics Express, 2019, 27, 26940.	3.4	24
107	Scene-based nonuniformity correction method using multiscale constant statistics. Optical Engineering, 2011, 50, 1.	1.0	23
108	Programmable Colored Illumination Microscopy (PCIM): A practical and flexible optical staining approach for microscopic contrast enhancement. Optics and Lasers in Engineering, 2016, 78, 35-47.	3.8	23

#	Article	IF	CITATIONS
109	Registration method for infrared images under conditions of fixed-pattern noise. Optics Communications, 2012, 285, 2293-2302.	2.1	22
110	Motion-oriented high speed 3-D measurements by binocular fringe projection using binary aperiodic patterns. Optics Express, 2017, 25, 540.	3.4	22
111	Real-time complex amplitude reconstruction method for beam quality M^2 factor measurement. Optics Express, 2017, 25, 20142.	3.4	22
112	Range limited double-thresholds multi-histogram equalization for image contrast enhancement. Optical Review, 2015, 22, 246-255.	2.0	20
113	3D Imaging Based on Depth Measurement Technologies. Sensors, 2018, 18, 3711.	3.8	20
114	Real-time microscopic 3D shape measurement based on optimized pulse-width-modulation binary fringe projection. Measurement Science and Technology, 2017, 28, 075010.	2.6	19
115	Single-shot color object reconstruction through scattering medium based on neural network. Optics and Lasers in Engineering, 2021, 136, 106310.	3.8	19
116	A two-frame approach for scene-based nonuniformity correction in array sensors. Infrared Physics and Technology, 2013, 60, 190-196.	2.9	18
117	Resolution-enhanced intensity diffraction tomography in high numerical aperture label-free microscopy. Photonics Research, 2020, 8, 1818.	7.0	18
118	Multimodal computational microscopy based on transport of intensity equation. Journal of Biomedical Optics, 2016, 21, 1.	2.6	17
119	Quantitative Phase Imaging Camera With a Weak Diffuser. Frontiers in Physics, 2019, 7, .	2.1	17
120	Has 3D finally come of age? ——An introduction to 3D structured-light sensor. Hongwai Yu Jiguang Gongcheng/Infrared and Laser Engineering, 2020, 49, 303001-303001.	0.4	17
121	Iterative optimum frequency combination method for high efficiency phase imaging of absorptive objects based on phase transfer function. Optics Express, 2015, 23, 28031.	3.4	16
122	Multi-step phase aberration compensation method based on optimal principal component analysis and subsampling for digital holographic microscopy. Applied Optics, 2019, 58, 389.	1.8	16
123	Dual-mode phase and fluorescence imaging with a confocal laser scanning microscope. Optics Letters, 2018, 43, 5689.	3.3	16
124	A carrier removal technique for Fourier transform profilometry based on principal component analysis. Optics and Lasers in Engineering, 2015, 74, 80-86.	3.8	15
125	Optimal wavelength selection strategy in temporal phase unwrapping with projection distance minimization. Applied Optics, 2018, 57, 2352.	1.8	15
126	Light field moment imaging: comment. Optics Letters, 2014, 39, 654.	3.3	14

#	Article	IF	CITATIONS
127	Two-dimensional stitching interferometry based on tilt measurement. Optics Express, 2018, 26, 23278.	3.4	13
128	Multiobjective Location Model Design Based on Government Subsidy in the Recycling of CDW. Mathematical Problems in Engineering, 2017, 2017, 1-9.	1.1	12
129	High-dynamic-range 3D shape measurement based on time domain superposition. Measurement Science and Technology, 2019, 30, 065004.	2.6	12
130	Wide-field anti-aliased quantitative differential phase contrast microscopy. Optics Express, 2018, 26, 25129.	3.4	12
131	Fourier Ptychographic Microscopy: Theory, Advances, and Applications. Guangxue Xuebao/Acta Optica Sinica, 2016, 36, 1011005.	1.2	12
132	Active depth estimation from defocus using a camera array. Applied Optics, 2018, 57, 4960.	1.8	11
133	Dynamic 3D measurement of thermal deformation based on geometric-constrained stereo-matching with a stereo microscopic system. Measurement Science and Technology, 2019, 30, 125007.	2.6	11
134	Upregulation of miR-150-5p alleviates LPS-induced inflammatory response and apoptosis of RAW264.7 macrophages by targeting Notch1. Open Life Sciences, 2020, 15, 544-552.	1.4	11
135	Single-exposure 3D label-free microscopy based on color-multiplexed intensity diffraction tomography. Optics Letters, 2022, 47, 969.	3.3	11
136	Comparative assessment of astigmatism-corrected Czerny-Turner imaging spectrometer using off-the-shelf optics. Optics Communications, 2017, 388, 53-61.	2.1	10
137	High-sensitive ultrasonic sensor using fiber-tip PVC diaphragm Fabry-Perot interferometer and its imaging application. Sensors and Actuators A: Physical, 2018, 279, 474-480.	4.1	10
138	Calibration and rectification of bi-telecentric lenses in Scheimpflug condition. Optics and Lasers in Engineering, 2022, 149, 106793.	3.8	10
139	Generation of Photonic Hooks from Patchy Microcylinders. Photonics, 2021, 8, 466.	2.0	10
140	Multi-pitch self-calibration measurement using a nano-accuracy surface profiler for X-ray mirror metrology. Optics Express, 2020, 28, 23060.	3.4	10
141	Isolation and comparison of mesenchymal stem cell-like cells derived from human gastric cancer tissues and corresponding ovarian metastases. Molecular Medicine Reports, 2016, 13, 1788-1794.	2.4	9
142	A color-corrected strategy for information multiplexed Fourier ptychographic imaging. Optics Communications, 2017, 405, 406-411.	2.1	9
143	Accurate quantitative phase imaging by the transport of intensity equation: a mixed-transfer-function approach. Optics Letters, 2021, 46, 1740.	3.3	9
144	Optimization analysis of partially coherent illumination for refractive index tomographic microscopy. Optics and Lasers in Engineering, 2021, 143, 106624.	3.8	9

#	Article	IF	CITATIONS
145	DeepDensity: Convolutional neural network based estimation of local fringe pattern density. Optics and Lasers in Engineering, 2021, 145, 106675.	3.8	9
146	Composite deep learning framework for absolute 3D shape measurement based on single fringe phase retrieval and speckle correlation. JPhys Photonics, 2020, 2, 045009.	4.6	9
147	Non-Interferometric Phase Retrieval and Quantitative Phase Microscopy Based on Transport of Intensity Equation: A Review. Zhongguo Jiguang/Chinese Journal of Lasers, 2016, 43, 0609002.	1.2	9
148	Deep Learning Based Computational Imaging: Status, Challenges, and Future. Guangxue Xuebao/Acta Optica Sinica, 2020, 40, 0111003.	1.2	9
149	Accelerated Fourier ptychographic diffraction tomography with sparse annular <scp>LED</scp> illuminations. Journal of Biophotonics, 2022, 15, e202100272.	2.3	9
150	Autofocusing Algorithm for Pixel-Super-Resolved Lensfree On-Chip Microscopy. Frontiers in Physics, 2021, 9, .	2.1	8
151	Super-Resolution Imaging with Patchy Microspheres. Photonics, 2021, 8, 513.	2.0	8
152	Intrapancreatic accessory spleen: Evaluation with CT and MRI. Experimental and Therapeutic Medicine, 2018, 16, 3623-3631.	1.8	7
153	Preliminary application of 125l–nivolumab to detect PD-1 expression in colon cancer via SPECT. Journal of Radioanalytical and Nuclear Chemistry, 2018, 318, 1237-1242.	1.5	7
154	Efficient single image stripe nonuniformity correction method for infrared focal plane arrays. Optical Review, 2012, 19, 355-357.	2.0	6
155	Single-shot spatial frequency multiplex fringe pattern for phase unwrapping using deep learning. , 2020, , .		6
156	Deep Learning Enabled Scalable Calibration of a Dynamically Deformed Multimode Fiber. Advanced Photonics Research, 2022, 3, .	3.6	6
157	Scene based nonuniformity correction based on block ergodicity for infrared focal plane arrays. Optik, 2012, 123, 833-840.	2.9	5
158	Phase extraction for dual-wavelength phase-shift Fizeau interferometry in the presence of multi-beam interference. Optics Communications, 2017, 402, 489-497.	2.1	5
159	Enhancing single-shot fringe pattern phase demodulation using advanced variational image decomposition. Journal of Optics (United Kingdom), 2019, 21, 045702.	2.2	5
160	Low-Light-Level Image Super-Resolution Reconstruction Based on a Multi-Scale Features Extraction Network. Photonics, 2021, 8, 321.	2.0	5
161	Microscopic fringe projection profilometry systems in Scheimpflug condition and performance comparison. Surface Topography: Metrology and Properties, 2022, 10, 024004.	1.6	5
162	Exploiting optical degrees of freedom for information multiplexing in diffractive neural networks. Light: Science and Applications, 2022, 11, .	16.6	5

#	Article	IF	CITATIONS
163	Comparison of Digital Holography and Transport of Intensity for Quantitative Phase Contrast Imaging. , 2014, , 137-142.		4
164	Arsenite Increases Linc-ROR in Human Bronchial Epithelial Cells that Can Be Inhibited by Antioxidant Factors. Biological Trace Element Research, 2020, 198, 131-141.	3.5	4
165	Real-time binocular stereo vision system based on FPGA. , 2018, , .		4
166	Absorption and phase decoupling in transport of intensity diffraction tomography. Optics and Lasers in Engineering, 2022, 156, 107082.	3.8	4
167	A commercialized digital holographic microscope with complete software supporting. , 2020, , .		4
168	Transport of intensity equation: a new approach to phase and light field. , 2014, , .		3
169	10.6μm Infrared light photoinduced insulator-to-metal transition in vanadium dioxide. Infrared Physics and Technology, 2014, 64, 103-107.	2.9	3
170	Automatic high order aberrations correction for digital holographic microscopy based on orthonormal polynomials fitting over irregular shaped aperture. Journal of Optics (United Kingdom), 2019, 21, 045609.	2.2	3
171	An auto-focusing reflection-type lens-less digital holographic microscope. , 2021, , .		3
172	Real-time three-dimensional infrared imaging using fringe projection prof ilometry. Chinese Optics Letters, 2013, 11, S21101-321104.	2.9	3
173	Application of deep learning technology to fringe projection 3D imaging. Hongwai Yu Jiguang Gongcheng/Infrared and Laser Engineering, 2020, 49, 303018-303018.	0.4	3
174	New developments in transport of intensity equation for phase retrieval and computational imaging. , 2014, , .		2
175	Spectrum aliasing minimization for Fourier ptychographic microscopy based on annular illumination optimization. , 2021, , .		2
176	Calibration of telecentric cameras with distortion center estimation. , 2018, , .		2
177	Bi-frequency temporal phase unwrapping using deep learning. , 2019, , .		2
178	High-speed in vitro intensity diffraction tomography. , 2019, , .		2
179	Video-rate quantitative phase microscopy based on Fourier ptychography with annular illuminations. , 2018, , .		2
180	Review of the development of differential phase contrast microscopy. Hongwai Yu Jiguang Gongcheng/Infrared and Laser Engineering, 2019, 48, 603014.	0.4	2

#	Article	IF	CITATIONS
181	Lens-free on-chip microscopy: theory, advances, and applications. Hongwai Yu Jiguang Gongcheng/Infrared and Laser Engineering, 2019, 48, 603009.	0.4	2
182	High dynamic range and real-time 3D measurement based on a multi-view system. , 2020, , .		2
183	Learning-based absolute 3D shape measurement based on single fringe phase retrieval and speckle correlation. , 2020, , .		2
184	SNR Improvement in Three-Step Phase Shifting Profilometry. , 2012, , .		1
185	Scene-Based Nonuniformity Correction with Multiframe Registration. , 2012, , .		1
186	Lensless transport-of-intensity phase microscopy and tomography with a color LED matrix. , 2015, , .		1
187	Quantitative phase measurement for wafer-level optics. , 2015, , .		1
188	Phase retrieval in arbitrarily shaped aperture with the transport-of-intensity equation. Proceedings of SPIE, 2015, , .	0.8	1
189	Coded multi-angular illumination for Fourier ptychography based on Hadamard codes. , 2015, , .		1
190	Computational microscopy with programmable illumination and coded aperture. , 2017, , .		1
191	A simplified imaging model of bi-telecentric lenses under Scheimpflug condition and its calibration. , 2021, , .		1
192	Quantitative weak phase approximation analysis of quantitative phase imaging based on asymmetric illumination. , 2021, , .		1
193	Pixel super resolution imaging method based on coded aperture modulation. , 2021, , .		1
194	super resolution reconstruction of low light level image based on the feature extraction convolution neural network. , 2021, , .		1
195	An openCL-based speckle matching on the monocular 3D sensor using speckle projection. , 2021, , .		1
196	Quantitative phase imaging camera with a weak diffuser based on the transport of intensity equation. , 2019, , .		1
197	NONUNIFORMITY CORRECTION FOR INFRARED FOCAL PLANE ARRAYS BASED ON ENVIRONMENTAL TEMPERATURE. Hongwai Yu Haomibo Xuebao/Journal of Infrared and Millimeter Waves, 2010, 29, 49-52.	0.2	1
198	Real-Time Three-Dimensional Measurement Composite of Epipolar Constraint and Speckle Correlation. Guangxue Xuebao/Acta Optica Sinica, 2016, 36, 1012003.	1.2	1

#	Article	IF	CITATIONS
199	Three dimensional micro surface measurement system based on stereomicroscope. Journal of Applied Optics, 2017, 38, 607-611.	0.2	1
200	Micro Fourier Transform Profilometry (μFTP): 3D imaging at 10,000 fps. , 2018, , .		1
201	System Calibration for Panoramic 3D Measurement with Plane Mirrors. Lecture Notes in Computer Science, 2019, , 15-26.	1.3	1
202	Transport-of-intensity equation (TIE) based phase imaging in a confocal laser scanning microscope. , 2019, , .		1
203	Three-dimensional tomographic microscopy technique with multi-frequency combination with partially coherent illuminations. , 2019, , .		1
204	The optimization criteria for resolution improvement in a lens-free on-chip digital holographic microscope. , 2019, , .		1
205	Video-rate isotropic quantitative differential phase contrast microscopy based on color-multiplexed annular illumination. , 2019, , .		1
206	High-speed 3D shape measurement with the multi-view system using deep learning. , 2019, , .		1
207	High-speed 3D measurements at 20,000Hz with deep convolutional neural networks. , 2019, , .		1
208	A computational super-resolution technique based on coded aperture imaging. , 2020, , .		1
209	Lensfree super-resolved microscopy based on multi-wavelength multiplexing. , 2020, , .		1
210	Optimal annular illumination pattern for Fourier ptychographic microscopy based on spectrum aliasing minimization. , 2020, , .		1
211	An iterative compensation solution to the transport-of-intensity equation. , 2020, , .		1
212	Three dimensional confocal photoacoustic dermoscopy with an autofocusing sonoâ€opto probe. Journal of Biophotonics, 2022, , e202100323.	2.3	1
213	Single-shot quantitative phase microscopy with the transport-of-intensity equation. Proceedings of SPIE, 2013, , .	0.8	0
214	Quantitative phase from defocused intensity by image deconvolution. , 2013, , .		0
215	Real-time 3D measurement based on structured light illumination considering camera lens distortion. Proceedings of SPIE, 2014, , .	0.8	0
216	Digital holography to light field. Proceedings of SPIE, 2014, , .	0.8	0

#	Article	IF	CITATIONS
217	Optimized dithering technique for 3D shape measurement based on intensity residual error. Proceedings of SPIE, 2014, , .	0.8	0
218	Phase space representation of transport of intensity phase retrieval for partially coherent fields. , 2014, , .		0
219	Silicon wafer microstructure imaging using InfraRed Transport of Intensity Equation. , 2015, , .		0
220	Phase-space analysis of transport of intensity equation under partially coherent illumination. , 2015, , .		0
221	Optimized multiplexing super resolution imaging based on a Fourier ptychographic microscope. , 2015, ,		Ο
222	Principal component analysis based carrier removal approach for Fourier transform profilometry. , 2015, , .		0
223	Optimum defocus planes selection method for transport of intensity phase imaging based on phase transfer function. Proceedings of SPIE, 2015, , .	0.8	Ο
224	Software design of a digital holographic microscope based on MFC, multi-document and multi-thread. Proceedings of SPIE, 2015, , .	0.8	0
225	A compact and lensless digital holographic microscope setup. , 2015, , .		Ο
226	GPU-assisted real-time three dimensional shape measurement by speckle-embedded fringe. , 2015, , .		0
227	A carrier removal approach for fringe projection profilometry using principal component analysis. , 2015, , .		Ο
228	Spatial-spectral data redundancy requirement for Fourier ptychographic microscopy. Proceedings of SPIE, 2016, , .	0.8	0
229	Computational method for multi-modal microscopy based on transport of intensity equation. Proceedings of SPIE, 2017, , .	0.8	Ο
230	Practical considerations for high speed real-time 3D measurements by the fringe projection. Proceedings of SPIE, 2017, , .	0.8	0
231	A positional misalignment correction method for Fourier ptychographic microscopy based on simulated annealing. , 2017, , .		О
232	The importance of the boundary condition in the transport of intensity equation based phase measurement. , 2017, , .		0
233	Three-dimensional measurement based on a Greenough-type stereomicroscope using phase-shifting projection. Proceedings of SPIE, 2017, , .	0.8	0
234	Multi-view phase unwrapping with composite fringe patterns. Proceedings of SPIE, 2017, , .	0.8	0

#	Article	IF	CITATIONS
235	High speed 3D shape measurements with motion compensation. Proceedings of SPIE, 2017, , .	0.8	0
236	Phase retrieval in moir $ ilde{A}$ © volume computed tomography based on spatial phase shifting by triple-crossed gratings. Applied Optics, 2017, 56, 9341.	1.8	0
237	High-frequency enhanced based on high-resolution synthetic spectrum quantitative phase imaging. , 2021, , .		0
238	Color deep learning profilometry for single-shot 3D shape measurement. , 2021, , .		0
239	An improved reliability-guided phase unwrapping algorithm for digital holographic microscopic. , 2021, , .		0
240	Super-resolution lensless microscopy using multi-wavelength multiplexing. , 2021, , .		0
241	Super-resolution simulation of terahertz coded aperture imaging. , 2021, , .		0
242	Accurate quantitative phase imaging by the transport of intensity equation: a mixed-transfer-function approach: erratum. Optics Letters, 2021, 46, 2408.	3.3	0
243	Structured-light 3D shape measurements using deep learning. , 2021, , .		0
244	Corrigendum to "Transport of intensity equation: A tutorial―Optics and Lasers in Engineering, Volume 135 (2020) 106187. Optics and Lasers in Engineering, 2021, , 106672.	3.8	0
245	Editorial: Optical Microscopic and Spectroscopic Techniques Targeting Biological Applications. Frontiers in Physics, 2021, 9, .	2.1	0
246	End-to-end single-shot composite fringe projection profilometry based on deep learning. , 2021, , .		0
247	Phase space retrieval by iterative three-dimensional intensity projections. , 2021, , .		0
248	Quantitative phase imaging with mixed-transfer-function for resolution enhancement. , 2021, , .		0
249	Super-resolution algorithm for lensless microscope based on z-axis correction. , 2021, , .		0
250	Nonuniformity Correction Based on Unified Photoresponse Characteristics of Infrared Focal Plane Arrays. Guangzi Xuebao/Acta Photonica Sinica, 2011, 40, 926-932.	0.3	0
251	Laplacian reconstruction of one single hologram using two dif ferent reconstruction distances or wavelengths. Chinese Optics Letters, 2012, 10, S10901-310904.	2.9	0
252	High dynamic range three-dimensional measurement using fringe projection technique. , 2014, , .		0

#	Article	IF	CITATIONS
253	Theory and Systematic Design of Rheinberg Illumination Microscopy Based on Programmable LCD. Guangxue Xuebao/Acta Optica Sinica, 2016, 36, 0818002.	1.2	0
254	Transmission Stereo Microscope Based on Programmable LED Array Illumination. Guangxue Xuebao/Acta Optica Sinica, 2016, 36, 0511005.	1.2	0
255	Lensless Imaging Method for Pinhole Type Point Diffraction Interferometer. Guangxue Xuebao/Acta Optica Sinica, 2017, 37, 0312002.	1.2	Ο
256	Multimodal quantitative phase and fluorescence imaging of cell apoptosis. , 2017, , .		0
257	Improved bi-frequency scheme to realize high-precision 3D shape measurement. , 2017, , .		Ο
258	Microscopic 3D measurement of dynamic scene using optimized pulse-width-modulation binary fringe. , 2017, , .		0
259	Pixel-resolution and image quality improvement in lensfree holographic microscopy using adaptive relaxation and positional error correction. , 2017, , .		Ο
260	An efficient iterative super-resolution technology for coded aperture imaging. , 2017, , .		0
261	Computational diffraction tomographic microscopy with transport of intensity equation using a light-emitting diode array. , 2017, , .		0
262	Fast 3D shape measurements with reduced motion artifacts. , 2017, , .		0
263	Resolution-improved Fourier ptychographic microscopy using high-numerical-aperture condenser. , 2017, , .		0
264	Pixel-super-resolved lensfree holography using adaptive relaxation factor and positional error correction. , 2018, , .		0
265	Robust stereo phase unwrapping based on a quad-camera system. , 2018, , .		0
266	Motion-compensated three-step phase-shifting profilometry. , 2018, , .		0
267	Effcient quantitative phase imaging for programmable LED light microscopy. , 2018, , .		0
268	The dynamic super-resolution phase imaging based on low-cost lensfree system. , 2018, , .		0
269	High-speed three-dimensional shape measurement using improved bi-frequency scheme and number-theoretical phase unwrapping. , 2018, , .		Ο
270	Adaptive denoising method based on iterative process for Fourier ptychographic microscopy. , 2018, , .		0

#	Article	IF	CITATIONS
271	High-speed 3D shape measurement using composite structured-light patterns and multiview system. , 2018, , .		0
272	3D imaging based on depth measurement. Hongwai Yu Jiguang Gongcheng/Infrared and Laser Engineering, 2019, 48, 603013.	0.4	0
273	Review of the development and application of deformation measurement based on digital holography and digital speckle interferometry. Hongwai Yu Jiguang Gongcheng/Infrared and Laser Engineering, 2019, 48, 603010.	0.4	0
274	Fast Stereo 3D Imaging Based on Random Speckle Projection and Its FPGA Implementation. Lecture Notes in Computer Science, 2019, , 205-216.	1.3	0
275	Robust Dynamic 3D Shape Measurement with Hybrid Fourier-Transform Phase-Shifting Profilometry. Lecture Notes in Computer Science, 2019, , 122-133.	1.3	0
276	Real-time 3D point cloud registration. , 2019, , .		0
277	High dynamic range and fast 3D measurement based on a telecentric stereo-microscopic system. , 2019, ,		0
278	High-speed three-dimensional shape measurement based on robust Gray-code coding strategies. , 2019, ,		0
279	Full-surface 3-D reconstruction based on surround structured lighting. , 2019, , .		0
280	Speckle quantitative phase imaging based on coherence eï $\neg \in$ ect compensation. , 2019, , .		0
281	Improved multi-slice Fourier ptychographic microscopy technique for high-accuracy three-dimensional tomography under oblique illuminations. , 2019, , .		0
282	Fast panoramic 3D shape measurement using the multi-view system with plane mirrors. , 2019, , .		0
283	Isotropic quantitative phase imaging with optimal differential phase contrast illumination scheme. , 2019, , .		0
284	Temporal phase unwrapping using multi-scale deep neural networks. , 2019, , .		0
285	Quantitative phase microscopy based on color-multiplexed single-shot Fourier ptychography. , 2019, , .		0
286	Single-shot 3D shape measurement with spatial frequency multiplexing using deep learning. , 2019, , .		0
287	Microscopic fringe projection profilometry comparison based on stereoscopic microscope and telecentric lenses. , 2019, , .		0
288	10.1063/1.5124535.1., 2019,,.		0

#	Article	IF	CITATIONS
289	Low-light-level image pixel super-resolution reconstruction method. , 2021, , .		Ο
290	Single-exposure 3D label-free microscopy based on color-multiplexed intensity diffraction tomography. , 2021, , .		0
291	Deep learning-based single-shot spatial frequency multiplexing composite fringe projection profilometry. , 2021, , .		0
292	High-accuracy real-time omnidirectional 3D scanning and inspection system. , 2021, , .		0
293	Calibration method for monocular 3D imaging systems based on reference planes. , 2021, , .		0
294	Fast and high-precision 3D face scanning system based on infrared fringe projection. , 2021, , .		0
295	Wide field coded aperture super resolution imaging. , 2021, , .		0
296	Speckle quantitative phase imaging camera based on the transport of intensity equation. , 2019, , .		0
297	Computational microscopy for quantitative phase imaging and refractive index tomography using annular illumination. , 2020, , .		0
298	Fast 3D measurement method based on improved digital image correlation using grid-based feature extraction. , 2021, , .		0
299	Optimizing design of partially coherent illumination for refractive index tomographic microscopy. , 2021, , .		0
300	Transport of intensity equation: noninterferometic phase imaging and diffraction tomography. , 2021, ,		0
301	Single-shot, 360-degree, and high-precision three- dimensional shape measurement for human heads based on digital image correlation and plane mirrors. , 2021, , .		0
302	Label-free quantitative 3D intensity diffraction tomographic imaging in high numerical aperture microscopy. , 2020, , .		0
303	Fast 3D surface defect detection with fringe projection. , 2020, , .		0
304	Stereo phase unwrapping method based on feedback projection. , 2020, , .		0
305	Optimization method for the synthetic apertures imaging system. , 2020, , .		0
306	Phase space retrieval and the imaging system effect. , 2020, , .		0

#	Article	IF	CITATIONS
307	Coherence eï¬ $\in$ ect compensation in diï¬ $\in$ user-based quantitative phase imaging. , 2020, , .		Ο
308	Anti-aliasing high resolution quantitative phase microscopy based on differential phase contrast imaging. , 2020, , .		0
309	Holographic lensless quantitative phase imaging microscope. , 2020, , .		0
310	Robust absolute 3D measurement using stereo cost-volume filtering for fringe orders. , 2020, , .		0
311	Miniaturized multi-contrast quantitative phase imaging microscope. , 2020, , .		Ο
312	Resolution-enhanced quantitative phase imaging from transport of intensity equation: mixed-transfer-function. , 2021, , .		0
313	Low-light-level image super-resolution reconstruction via deep learning network. , 2021, , .		Ο
314	Stereo rectification of Scheimpflug telecentric lenses. , 2021, , .		0
315	Coherence retrieval via three-dimensional intensity measurement. , 2021, , .		0
316	Stereo phase unwrapping using deep learning for single-shot absolute 3D shape measurement. , 2021, , .		0
317	Learning-based 3D shape measurements with fringe projection. , 2020, , .		0
318	Deep-learning-enabled fringe projection profilometry. , 2020, , .		0
319	Pixel-super-resolution lensfree microscopy based on multiple-wavelength scanning. , 2020, , .		Ο
320	Wigner distribution function retrieval via three-dimensional intensity measurement. , 2020, , .		0
321	Learning-based absolute 3D shape measurement based on single fringe phase retrieval and speckle correlation. , 2020, , .		Ο
322	Super resolution imaging method based on the synthetic aperture system. , 2020, , .		0
323	3D resolution-enhanced intensity diffraction tomographic microscopy. , 2020, , .		0
324	Improved multi-slice Fourier ptychographic diffraction tomography based on high-numerical-aperture illuminations. , 2020, , .		0

#	Article	IF	CITATIONS
325	Transport of intensity diffraction tomography with non-interferometric synthetic aperture. , 2022, , .		О
326	Accelerated Fourier ptychographic diffraction tomography based on coded illumination. , 2022, , .		0